Steel and Composite Structures, *Vol. 15, No. 1 (2013) 57-79*
DOI: http://dx.doi.org/10.12989/scs.2013.15.1.057

Dynamic stability analysis of laminated composite plates in thermal environments

Chun-Sheng Chen[1], Ting-Chiang Tsai[2], Wei-Ren Chen[*3] and Ching-Long Wei[1]

[1] *Department of Mechanical Engineering, Lunghwa University of Science and Technology, Guishan Shiang 33306, Taiwan*
[2] *Department of Mechanical Engineering, National Taipei University of Technology, Taipei 10608, Taiwan*
[3] *Department of Mechanical Engineering, Chinese Culture University, Taipei 11114, Taiwan*

(Received March 31, 2011, Revised April 29, 2013, Accepted June 04, 2013)

Abstract. This paper studies the dynamic instability of laminated composite plates under thermal and arbitrary in-plane periodic loads using first-order shear deformation plate theory. The governing partial differential equations of motion are established by a perturbation technique. Then, the Galerkin method is applied to reduce the partial differential equations to ordinary differential equations. Based on Bolotin's method, the system equations of Mathieu-type are formulated and used to determine dynamic instability regions of laminated plates in the thermal environment. The effects of temperature, layer number, modulus ratio and load parameters on the dynamic instability of laminated plates are investigated. The results reveal that static and dynamic load, layer number, modulus ratio and uniform temperature rise have a significant influence on the thermal dynamic behavior of laminated plates.

Keywords: dynamic instability; laminated plates; Bolotin's method; temperature

1. Introduction

Laminated composite plates have been used successfully in many engineering applications because they have better strength and modulus over traditional metal plates. During the operational life of typical engineering structures, elevated temperature acting throughout the laminated composite plates may be experienced. Due to this high temperature condition, thermolelastic properties of the composite plates will vary with the change of temperature and compressive stresses acting on the edges of the plates are induced. Meanwhile, a periodic in-plane load sometimes acting on a plate, may lead to the parametrically excited dynamic instability phenomenon. Thus, the study of dynamic stability behavior of laminated composite plates in thermal environments is of considerable importance in plate design engineering. Numerous references pertaining to the parametric resonance of plates can be found in the books by Bolotin (1964) and Evan-Ivanowski (1976). For the past years, the dynamic stability of laminate composite plates has been studied by many researchers using various approximate methods (Dey and Sinqha (2006), Chakrabarti (2008), Chen *et al*. (2009), Patel *et al*. (2009)).

To efficiently use laminated composite plates in thermal environments, a good understanding of dynamic behavior for laminated composite plates under varying thermal conditions is needed. A

∗Corresponding author, Associate Professor, E-mail: wrchen@faculty.pccu.edu.tw

http://www.techno-press.org/?journal=scs&subpage=8 ISSN: 1229-9367 (Print), 1598-6233 (Online)

number of investigations dealing with thermal dynamic response of composite plate had been presented in the published literature. Makhecha *et al*. (2001) studied the realistic variation of displacements through the thickness for the dynamic response analysis of laminated plates. The influence of ply angle, aspect ratio, number of layers and thermal coefficient on the dynamic response of laminates was investigated. Shukla and Nath (2002) presented the dynamic buckling of laminated plates subjected to the time-dependent thermal-induced in-plane loading. The dynamic post-buckling deflection response was obtained and dynamic critical temperatures were estimated. The dynamic response of laminated plates exposed to thermomechanical loading and resting on an elastic foundation was analyzed by Shen *et al*. (2003). Analytical solutions of dynamic response for laminated plates under a transverse dynamic load and a uniform temperature rise were obtained. Effects of foundation stiffness, side-to-thickness ratio and temperature rise on the dynamic response were studied. Tylikowski (2003) dealt with the dynamics of laminated plates under uniform space and time-dependent temperature fields. The thermally induced instability and the dynamic thermal buckling of laminated plates were investigated theoretically.

The dynamic thermoelastic response of a heated composite plate was investigated by Al-Huniti and Al-Nimr (2004). The plate was heated by a step-function heat source generated within the matrix. The spatial and time variation of the temperature were calculated and presented. Heidary and Eslami (2004) derived equations governing the dynamic response of a piezothermoelastic laminated plate based on the first-order shear deformation theory. The thermal loading and piezoelectric control analysis were solved using the time marching method. The displacements caused by temperature change are important in the precision sensing and control of distributed systems by piezoelectric materials. Fares *et al*. (2004) presented an optimal laminate dynamic response of cross-ply laminate plate under thermomechanical loadings. The optimization procedure aims to maximize the temperature, and to minimize the dynamic response subject to constraints on the thickness and control energy. The dynamic buckling of imperfect piezolaminated plates under suddenly applied thermal and mechanical loads was investigated by Shariyat (2009). Complex dynamic loading combinations of in-plane mechanical loads, heating and electrical actuations were considered. Moradi and Mansouri (2012) investigated the thermal buckling of composite laminated plates under a uniform temperature distribution based on the differential quadrature method. The influences of the aspect ratio, fiber orientation, modulus ratio, and restraint conditions on the critical temperature were studied. Thermal buckling load optimization of laminated plates with various intermediate line supports was studied by Topal (2012). The effects of the location of line supports, aspect ratios and boundary conditions on the critical thermal buckling load were investigated.

To the best of our knowledge, there exists no literature concerning the dynamic stability of laminated composite plate subjected to an arbitrary dynamic load in the thermal environment. In the present study, the governing equations of laminated plates subjected to an arbitrary dynamic load and a thermal environment are established by using the perturbation technique. The temperature field is assumed to be a combination of uniform and linear temperature distribution along the plate thickness. The dynamic load is taken to be a combination of a periodic bending stress and axial stress in the example problems. The Galerkin method is applied to reduce the governing partial differential equations to ordinary differential equations. By using the Bolotin's method, the Mathieu equations are formed and used to determine the regions of dynamic instability of laminated plates. The effects of load parameters, layer number, temperature rise and modulus ratio on the dynamic instability regions and dynamic instability index of laminated plates are investigated.

2. Theoretical formulations

Following a similar technique by Chen (2007), the governing equations of motion of the initially stressed laminate composite plate in thermal condition are established using a perturbation technique. The governing equation can be expressed as

$$(\sigma_{ij}\overline{u}_{sj})_{,i} + \overline{\sigma}_{is,i} + \overline{F}_s + \Delta F_s = \rho\ddot{\overline{u}}_s \tag{1}$$

where σ_{ij}, $\overline{\sigma}_{is}$, $\overline{u}_s$, $\overline{F}_s$ and ΔF_s are the initial stress, perturbing stress, displacement, perturbing body force and body force, respectively.

In this paper, a first-order shear deformation plate theory is used to analyze the dynamic behavior of laminated composite plates. Both effects of rotary inertia and transverse shear deformation are taken into account. Thus, the incremental displacements are assumed to be of the forms.

$$\begin{aligned} u(x,y,z,t) &= u_x(x,y,t) + z\varphi_x(x,y,t) \\ v(x,y,z,t) &= u_y(x,y,t) + z\varphi_y(x,y,t) \\ w(x,y,z,t) &= u_z(x,y,t) \end{aligned} \tag{2}$$

Here u_x, u_y and w are displacements at the midplane in the x, y and z directions, respectively; φ_x and φ_y are rotation angles about y and x axes, respectively. The x and y axes of the coordinates are set to coincide with the two edges of the rectangular laminate plate. The constitutive relationship for a kth lamina accounting for the thermal effect is given by

$$\begin{bmatrix} \overline{\sigma}_{xx} \\ \overline{\sigma}_{yy} \\ \overline{\sigma}_{xy} \\ \overline{\sigma}_{yx} \\ \overline{\sigma}_{zx} \end{bmatrix}^{(k)} = \begin{bmatrix} C_{11} & C_{12} & C_{16} & 0 & 0 \\ C_{12} & C_{22} & C_{26} & 0 & 0 \\ C_{16} & C_{26} & C_{66} & 0 & 0 \\ 0 & 0 & 0 & C_{44} & C_{45} \\ 0 & 0 & 0 & C_{45} & C_{55} \end{bmatrix}^{(k)} \begin{bmatrix} \overline{\varepsilon}_{xx} - \alpha_{xx}\Delta T \\ \overline{\varepsilon}_{yy} - \alpha_{yy}\Delta T \\ \overline{\varepsilon}_{xy} - \alpha_{xy}\Delta T \\ \overline{\varepsilon}_{yx} \\ \overline{\varepsilon}_{zx} \end{bmatrix} \tag{3}$$

In this study, we consider a rectangular laminated plate of uniform thickness h subjected to an arbitrary time-dependent initial stress. The arbitrary dynamic load is assumed to have the form

$$\begin{aligned} \sigma_{ij} &= \sigma_{ij}^{n} + \frac{2z\sigma_{ij}^{m}}{h} \\ &= \left(\sigma_{ij}^{S} + \sigma_{ij}^{D}\cos\varpi t\right) + \frac{2z\left(\sigma_{ij}^{Sm} + \sigma_{ij}^{Dm}\cos\varpi t\right)}{h} \quad (i,j = x,y,z) \end{aligned} \tag{4}$$

which consists of the spatially uniform longitudinal, transverse, shear, bending and twisting stress.

Here σ_{ij}^{S} and σ_{ij}^{D} denote the static and dynamic components of the periodic normal or shear stress; σ_{ij}^{Sm} and σ_{ij}^{Dm} are the static and dynamic components of the periodic pure bending or torsion stress; ϖ is the angular frequency of excitation. Substitute Eqs. (2)-(4) into Eq. (1), perform all necessary partial integrations and group terms together by the displacements variation to yield the

dynamic equations for the rectangular laminated plate as follows

$$\begin{aligned}&\left[\begin{array}{l}A_{11}u_{x,x}+A_{16}(u_{x,y}+u_{y,x})+A_{12}u_{y,y}+B_{11}\varphi_{x,x}+B_{16}(\varphi_{x,y}+\varphi_{y,x})\\+B_{12}\varphi_{y,y}+N_{xx}u_{x,x}+M_{xx}\varphi_{x,x}+N_{xy}u_{x,y}+M_{xy}\varphi_{x,y}+N_{xz}u_{z,x}\\+N^T_{xx}u_{x,x}+M^T_{xx}\varphi_{x,x}+N^T_{xy}u_{x,y}+M^T_{xy}\varphi_{x,y}\end{array}\right]_{,x}\\&+\left[\begin{array}{l}A_{16}u_{x,x}+A_{26}u_{y,y}+A_{66}(u_{x,y}+u_{y,x})+B_{16}\varphi_{x,x}+B_{66}(\varphi_{x,y}+\varphi_{y,x})\\+B_{26}\varphi_{y,y}+N_{yy}u_{x,y}+M_{yy}\varphi_{x,y}+N_{xy}u_{x,x}+M_{xy}\varphi_{x,x}+N_{yz}u_{z,x}\\+N^T_{yy}u_{x,y}+M^T_{yy}\varphi_{x,y}+N^T_{xy}u_{x,x}+M^T_{xy}\varphi_{x,x}\end{array}\right]_{,y}+f_x=I_1\ddot{u}_x\end{aligned}\tag{5}$$

$$\begin{aligned}&\left[\begin{array}{l}A_{16}u_{x,x}+A_{66}(u_{x,y}+u_{y,x})+A_{26}u_{y,y}+B_{16}\varphi_{x,x}+B_{66}(\varphi_{x,y}+\varphi_{y,x})\\+B_{26}\varphi_{y,y}+N_{xx}u_{y,x}+M_{xx}\varphi_{y,x}+N_{xy}u_{y,y}+M_{xy}\varphi_{y,y}+N_{xz}u_{z,y}\\+N^T_{xx}u_{y,x}+M^T_{xx}\varphi_{y,x}+N^T_{xy}u_{y,y}+M^T_{xy}\varphi_{y,y}\end{array}\right]_{,x}\\&+\left[\begin{array}{l}A_{12}u_{x,x}+A_{26}(u_{x,y}+u_{y,x})+A_{22}u_{y,y}+B_{12}\varphi_{x,x}+B_{26}(\varphi_{x,y}+\varphi_{y,x})\\+B_{22}\varphi_{y,y}+N_{yy}u_{y,y}+M_{yy}\varphi_{y,y}+N_{xy}u_{y,x}+M_{xy}\varphi_{y,x}+N_{xz}u_{z,y}\\+N^T_{yy}u_{y,y}+M^T_{yy}\varphi_{y,y}+N^T_{xy}u_{y,x}+M^T_{xy}\varphi_{y,x}\end{array}\right]_{,y}+f_x=\rho h\ddot{u}_x\end{aligned}\tag{6}$$

$$\begin{aligned}&\left[A_{55}(w_{,x}+\varphi_x)+A_{45}(w_{,y}+\varphi_y)+N_{xx}w_{,x}+N_{xy}w_{,y}+N^T_{xx}w_{,y}+N^T_{xy}w_{,y}\right]_{,x}\\&+\left[A_{45}(w_{,x}+\varphi_x)+A_{44}(w_{,y}+\varphi_y)+N_{xy}w_{,x}+N_{yy}w_{,y}+N^T_{xy}w_{,x}+N^T_{yy}w_{,y}\right]_{,y}+f_z=I_1\ddot{w}\end{aligned}\tag{7}$$

$$\begin{aligned}&\left[\begin{array}{l}B_{11}u_{x,x}+B_{16}(u_{x,y}+u_{y,x})+B_{12}\varphi_{y,y}+D_{11}\varphi_{x,x}+D_{16}(\varphi_{x,y}+\varphi_{y,x})\\+D_{12}\varphi_{y,y}+M_{xx}u_{x,x}+M^*_{xx}\varphi_{x,x}+M_{xy}u_{x,y}+M^*_{xy}\varphi_{x,y}+M_{xz}u_{z,x}\\+M^T_{xx}y_{x,x}+M^{T*}_{xx}\varphi_{x,x}+M^T_{xy}u_{x,y}+M^{T*}_{xy}\varphi_{x,y}\end{array}\right]_{,x}\\&+\left[\begin{array}{l}B_{16}u_{x,x}+B_{66}(u_{x,y}+u_{y,x})+B_{26}u_{y,y}+D_{16}\varphi_{x,x}+D_{66}(\varphi_{x,y}+\varphi_{y,x})\\+D_{22}\varphi_{y,y}+M_{yy}u_{x,y}+M^*_{yy}\varphi_{x,y}+M_{xy}u_{x,x}+M^*_{xy}\varphi_{x,x}+M_{yz}u_{z,x}\\+M^T_{yy}u_{x,y}+M^{T*}_{yy}\varphi_{x,y}+M^T_{xy}u_{x,x}+M^{T*}_{yy}u_{x,x}\end{array}\right]_{,y}\\&-A_{55}\left(w_{,x}+\varphi_x\right)-\left(N_{xz}u_{x,x}+M_{xz}\varphi_{x,x}+N_{zz}\varphi_x+N_{zy}u_{x,y}+M_{zy}\varphi_{x,y}\right)+m_x=I_3\ddot{\varphi}_x\end{aligned}\tag{8}$$

$$
\begin{aligned}
&\left[\begin{array}{l}
B_{13}u_{x,x}+B_{66}(u_{x,y}+u_{y,x})+B_{26}u_{y,y}+D_{16}\varphi_{x,x}+D_{66}(\varphi_{x,y}+\varphi_{y,x}) \\
+D_{26}\varphi_{y,y}+M_{xx}u_{y,x}+M^{*}_{xx}\varphi_{y,x}+M_{xy}u_{y,y}+M^{*}_{xy}\varphi_{y,y}+M_{xz}u_{z,y} \\
+M^{T}_{xx}y_{y,x}+M^{T*}_{xx}\varphi_{y,x}+M^{T}_{xy}u_{y,y}+M^{T*}_{xy}\varphi_{y,y}
\end{array}\right]_{,x} \\
&+\left[\begin{array}{l}
B_{26}(u_{x,x}+u_{y,x})+B_{12}u_{x,x}+B_{22}u_{y,y}+D_{12}\varphi_{x,x}+D_{26}(\varphi_{x,y}+\varphi_{y,x}) \\
+D_{22}\varphi_{y,y}+M_{yy}u_{y,y}+M^{*}_{yy}\varphi_{y,y}+M_{xy}u_{y,x}+M^{*}_{xy}\varphi_{y,x}+M_{xz}u_{z,y} \\
+M^{T}_{yy}u_{y,y}+M^{T*}_{yy}\varphi_{y,y}+M^{T}_{xy}u_{y,x}+M^{T*}_{xy}u_{y,x}
\end{array}\right]_{,y} \\
&-A_{44}\left(w_{,y}+\varphi_{y}\right)-\left(N_{xz}u_{y,x}+M_{xz}\varphi_{y,x}+N_{zz}\varphi_{y}+N_{zy}u_{y,y}+M_{zy}\varphi_{y,y}\right)+m_{x}=I_{3}\ddot{\varphi}_{y}
\end{aligned}
\tag{9}
$$

where

$$
\begin{aligned}
&\left(A_{ij},B_{ij},D_{ij}\right)=\int C_{ij}(1,z,z^{2})dz \quad (i,j=1,2,6) \\
&\left(A_{ij},B_{ij},D_{ij}\right)=\int \kappa C_{ij}(1,z,z^{2})dz \quad (i,j=4,5) \\
&\left(N_{ij},M_{ij},M^{*}_{ij}\right)=\int \sigma_{ij}(1,z,z^{2})dz \quad (i,j=x,y,z) \\
&\left(N^{T}_{ij},M^{T}_{ij},M^{T*}_{ij}\right)=\int \alpha_{ij}C_{ij}\Delta T(1,z,z^{2})dz \quad (i,j=x,y) \\
&\left(I_{1},I_{3}\right)=\int \rho(z)(1,z^{2})dz
\end{aligned}
\tag{10}
$$

Here C_{ij}'s are the elastic constants of the stiffness matrix; ρ is the mass density; A_{ij}, B_{ij} and D_{ij} are the laminate stiffness coefficients; κ is the shear correction factor; N_{ij}, M_{ij} and M^{*}_{ij} are arbitrary initial stress resultants; N^{T}_{ij}, M^{T}_{ij} and M^{*}_{jj} are thermally stress resultants; f_x, f_y, f_z, m_x and m_y are the lateral loadings. All the integrations are carried out through the thickness of the plate from $-h/2$ to $h/2$.

3. Numerical examples

Because there are so many parameters will affect the dynamic behavior of the laminated plate under an arbitrary dynamic load, it would be difficult to present results for all cases. In the following, the dynamic stability of the simply supported laminated composite plate subjected to the periodic spatially uniform longitudinal normal stress and pure bending stress and under a combined uniform and linear temperature rise in the thickness direction will be investigated. With all other stresses being zero, the stress system Eq. (4) is reduced to

$$\sigma_{xx}=\sigma_{n}+2z\sigma_{m}/h \tag{11}$$

with $\sigma_n=\sigma^{S}_{xx}+\sigma^{D}_{xx}\cos\varpi t=\sigma^{S}+\sigma^{D}\cos\varpi t$ and $\sigma_m=\sigma^{Sm}_{xx}+\sigma^{Dm}_{xx}\cos\varpi t=\sigma^{Sm}+\sigma^{Dm}\cos\varpi t$. The stress components σ^{S}, σ^{D}, σ^{Sm} and σ^{Dm} are taken to be constants. Thus, the only nonzero loads are $N_{xx}=h\sigma_n$, $M_{xx}=\beta h^{2}\sigma_m/6$, $M^{*}_{xx}=h^{3}\sigma_n/12$, where $\beta=\sigma_m/\sigma_n$ is the bending ratio of bending stress to normal stress.

The temperature distribution in the laminated plate is assumed to be a function of variable z along the plate thickness. Here, temperature rise is taken to be linear through the plate thickness as follows

$$\Delta T = T_o + 2zT_g$$

where T_o is the uniform temperature rise and T_g is the temperature gradient. As a result of the temperature difference within the plate, the plate may experience thermal compressive stresses as well as thermal bending stresses. Thus, the nonzero thermal stress resultants are $N_{ij}^{T} = -\alpha_{ij}C_{ij}T_o h$, $M_{ij}^{T} = -\alpha_{ij}C_{ij}T_g h^2 / 6$ and $M_{ij}^{T*} = -\alpha_{ij}C_{ij}T_o h^3 / 12$ $(i, j = x, y)$.

The conditions for boundary sides along $x = 0$ and a, $y = 0$ and b of the rectangular laminated composite plate are all simply supported. To satisfy the simply supported boundary conditions, the following shape modes of displacement fields are used.

$$\begin{aligned}
u_x &= \sum\sum h\, U_{mn}(t)\cos(m\pi x/a)\sin(n\pi y/b) \\
u_y &= \sum\sum h\, V_{mn}(t)\sin(m\pi x/a)\cos(n\pi y/b) \\
w &= \sum\sum h\, W_{mn}(t)\sin(m\pi x/a)\sin(n\pi y/b) \\
\varphi_x &= \sum\sum \Psi_{xmn}(t)\cos(m\pi x/a)\sin(n\pi y/b) \\
\varphi_y &= \sum\sum \Psi_{ymn}(t)\sin(m\pi x/a)\cos(n\pi y/b)
\end{aligned} \tag{12}$$

Assume that $\Delta_{(t)} = [U_{mn},\ V_{mn},\ W_{mn},\ \Psi_{xmn},\ \Psi_{ymn}]^T = \bar{\Delta} f(t)$, in which Δ and $\bar{\Delta}$ denote the time-dependent and time-independent displacement vector, respectively. Then, substituting the assumed displacement fields into governing Eqs. (5)-(9) and applying Galerkin method lead to the equations of motion in matrix form.

$$\left[\left(K - T + G\right)f(t) + M\left(\frac{d^2 f(t)}{dt}\right)\right]\bar{\Delta} = 0 \tag{13}$$

where K, T, G and M are the respective elastic stiffness matrix, thermal effect matrix, geometric stiffness matrix and mass matrix. The system Eq. (13) is related to the eigenvalue problems of the thermal buckling, static buckling stability, free vibration and dynamic instability.

To analyze the thermal buckling of laminated plates, the inertia term M and dynamic load term G are set to zero in Eq. (13). The eigenvalue equation now simplifies to

$$\left(K - T\right)\Delta = 0 \tag{14}$$

which can be used to obtain the thermal buckling temperature. The condition for the existence of the non-trivial solution is that the determinant of the coefficients should vanish. The critical buckling temperature rise T_{cr} can be determined as the solution

$$\left|K - T_{cr}T^*\right| = 0 \tag{15}$$

The eigenvalue equation for studying the free vibration of laminated plates without thermal effect can be obtained from Eq. (13) by setting $T = G = 0$ and $f(t) = e^{i\omega t}$

$$\left(K - \omega^2 M\right)\overline{\Delta} = 0 \tag{16}$$

The roots of the determinant of the coefficients of Eq. (16) are the natural frequencies of the laminated plate. By letting $T = 0$ and $f(t) = 1$ in Eq. (13), the static buckling problem for laminated plates without thermal influence can be formed as

$$\left(K - P_{cr}G^*\right)\overline{\Delta} = 0 \tag{17}$$

where P_{cr} is the static critical buckling load.

The dynamic stability analysis of the laminated plate under non-zero periodic stress as given in Eq. (11) is presented next. The nonzero stress resultant N_{xx} can be obtained by integrating Eq. (11) with respect to variable z as

$$N_{xx} = -\left(\alpha_s P_{cr} + \alpha_D P_{cr}\cos\varpi t\right) \tag{18}$$

where $\alpha_S = h\sigma_{xx}^S / P_{cr}$ and $\alpha_D = h\sigma_{xx}^D / P_{cr}$ are the static and dynamic load parameter, respectively. P_{cr} is the buckling load of the plate subjected to uniaxial in-plane load. Then, substituting Eq. (18) into Eq. (13) gives

$$\left[\left(K - T + \alpha_S P_{cr}G^* + \alpha_D P_{cr}G^*\cos\varpi t\right)f(t) + M\left(\frac{d^2 f(t)}{dt}\right)\right]\overline{\Delta} = 0 \tag{19}$$

Mathieu Eq. (19) represents the dynamic stability problem of a parametrically excited plate subjected to a periodic in-plane load. To determine the regions of dynamic instability, Bolotin's method (1964) is used. The boundaries of the dynamic instability regions can be constructed by the periodic solutions with period $2T$ and T respectively in Fourier series as

$$f(t)\overline{\Delta} = \sum_{k=1,3,5\ldots}^{\infty}\left(\mathbf{a_k}\sin\frac{k\varpi t}{2} + \mathbf{b_k}\cos\frac{k\varpi t}{2}\right) \tag{20}$$

$$f(t)\overline{\Delta} = \sum_{k=0,2,4\ldots}^{\infty}\left(\mathbf{a_k}\sin\frac{k\varpi t}{2} + \mathbf{b_k}\cos\frac{k\varpi t}{2}\right) \tag{21}$$

where a_k and b_k are arbitrary time invariant vectors. Substituting Eqs. (20) and (21) into Eq. (19) and separating the $\sin(k\varpi t / 2)$ and $\cos(k\varpi t / 2)$ parts, two sets of linear algebraic equations in a_k and b_k are obtained for each solution. Then, the boundaries between stable and unstable regions could be determined from the condition that the set of equations has nontrivial solutions. The determinant equation of infinite order for the dynamic stability boundaries with period $2T$ is given as

$$\begin{vmatrix} K + \alpha_S P_{cr}G \pm \frac{1}{2}\alpha_D P_{cr}G - \frac{1}{4}\varpi^2 M & \frac{1}{2}\alpha_D P_{cr}G & \cdots \\ \frac{1}{2}\alpha_D P_{cr}G & K + \alpha_S P_{cr}G - \frac{9}{4}\varpi^2 M & \cdots \\ \cdots & \cdots & \cdots \end{vmatrix} = 0 \tag{22}$$

For the period T the determinant equation of infinite dimension are

$$\begin{vmatrix} K+\alpha_S P_{cr} G-\varpi^2 M & \frac{1}{2}\alpha_D P_{cr} G & \cdots \\ \frac{1}{2}\alpha_D P_{cr} G & K+\alpha_S P_{cr} G-4\varpi^2 M & \cdots \\ \cdots & \cdots & \cdots \end{vmatrix} = 0 \tag{23}$$

and

$$\begin{vmatrix} K+\alpha_S P_{cr} G & \alpha_D P_{cr} G & \cdots \\ \alpha_D P_{cr} G & K+\alpha_S P_{cr} G-\varpi^2 M & \cdots \\ \cdots & \cdots & \cdots \end{vmatrix} = 0 \tag{24}$$

However, it is impossible to solve the determinant equations of infinite order to obtain the stability boundaries. To look for the stability boundaries, different orders of approximation can be used to obtain results which are sufficiently close approximations of the infinite determinant Eqs. (22)-(24). The boundaries of primary instability region with period $2T$ are usually much larger than those of secondary instability region with period T, and are therefore of greater practical importance. As the first-order approximation (a_1 and b_1) of the primary instability region with period $2T$ is capable of obtaining a sufficiently close approximation of the infinite eigenvalue problem (Chen and Yang (1990)), only the first-order solution of primary instability region will be presented in this study, which is given by

$$K+\alpha_S P_{cr} G \pm \tfrac{1}{2}\alpha_D P_{cr} G - \tfrac{1}{4}\varpi^2 M = 0 \tag{25}$$

4. Results and discussions

To check the accuracy of the present study, the critical temperatures, vibration and dynamic excitation frequencies of different laminate plates of the present model and those by other investigators are shown in Tables 1-3. It can be observed that the present results agree well with those obtained by Matsunaga (2005), Liu and Huang (1996) and Wang and Dawe (2002).

Table 1 Comparison of minimum critical temperatures of three-layer cross-ply laminated composite plate

a/h	Matsunaga (2005)	Present
20/10	0.3334	0.3438
20/6	0.2465	0.2554
20/5	0.2184	0.2216
20/4	0.1763	0.1802
20/3	0.1294	0.1299
20/2	0.0746	0.0731
20/1	0.0230	0.0219

Table 2 Comparison of vibration frequencies of a [0/90]s square plate in thermal environment

T_o		α_1 / α_2			
		-0.05	0.1	0.2	0.3
-50	Liu (1996)	15.149	15.247	15.320	15.394
	Present	15.165	15.277	15.351	15.425
0	Liu (1996)	15.150	15.150	15.150	15.150
	Present	15.179	15.179	15.179	15.179
50	Liu (1996)	15.164	15.052	14.978	14.902
	Present	15.193	15.081	15.006	14.930

Table 3 Excitation frequencies for a simply supported symmetrically four-layer cross-ply laminate plate with various static and dynamic loads

α_S	α_D	Wang (2002)		Present	
		ω^U	ω^L	ω^U	ω^L
0.0	0.0	144.57	144.57	144.36	144.36
0.0	0.3	155.03	133.29	155.64	133.79
0.0	0.6	164.83	120.95	165.12	121.45
0.0	0.9	174.08	107.21	174.43	107.63
0.0	1.2	182.87	91.43	183.21	91.86
0.0	1.5	191.25	72.28	191.75	72.62
0.2	0.06	131.71	126.86	132.12	127.26
0.4	0.12	117.45	106.24	117.96	106.82
0.6	0.18	101.20	80.49	101.84	81.10
0.8	0.24	81.78	40.89	82.31	41.32

The dynamic instability behaviors of the initially-stressed cross-ply laminate plates in thermal environmental condition will be investigated next, based on the procedure described in the previous section. The effects of various variables on dynamic instability will also be given and discussed. The non-dimensional coefficients of excitation frequency, $\Omega = \varpi b^2 \sqrt{\rho / h^2 E_2}$, the width of the instability region, $\Delta\Omega = \Omega^U - \Omega^L$ and the dynamic instability index, $\Omega_{DI} = \Delta\Omega / (\omega_{nf} K_{cr})$ are defined and used throughout the dynamic instability studies. Here Ω^U and Ω^L are the respective upper and lower boundary excitation frequency; $\omega_{nf} = \varpi b^2 \sqrt{\rho / h^2 E_2}$ and $K_{cr} = (N_{xx})_{cr} b^2 / E_2 h^4$ are the dimensionless fundamental natural frequency and critical buckling load. The dynamic instability index Ω_{DI} represents a relationship among the instability region, fundamental natural frequency and static critical buckling load, which is used as an instability measure of the laminate plates under thermal condition.

The effects of static and dynamic load parameter on the excitation frequency, instability region and dynamic instability index of laminated plates with various layer numbers in uniform temperature condition are presented in Tables 4-6 and Figs. 1-2. The static load parameter varies from 0 to 0.8 and the ratio of α_D / α_S is kept as 0.3. It can be seen that the increasing compressive

Table 4 Effect of layer number on the dynamic instability with different compressive static load parameters ($a/b = 1$, $a/h = 10$, $E_1 / E_2 = 40$, $T_o / T_{cr} = 0.5$, $\alpha_D / \alpha_S = 0.3$, $\beta = 0$)

N		α_S				
		0	0.2	0.4	0.6	0.8
2	Ω^U	15.0818	13.7402	12.2525	10.5573	8.5317
	Ω^L	15.0818	13.2342	11.0829	8.3973	4.2661
	$\Delta\Omega$	0	0.5059	1.1697	2.1600	4.2655
	Ω_{DI}	0	1.1645	2.6922	4.9716	9.8178
4	Ω^U	21.4231	19.5174	17.4043	14.9963	12.1189
	Ω^L	21.4231	18.7988	15.7428	11.9280	6.0597
	$\Delta\Omega$	0	0.7187	1.6615	3.0682	6.0592
	Ω_{DI}	0	0.5771	1.3343	2.4640	4.8658
6	Ω^U	22.2245	20.2475	18.0553	15.5572	12.5722
	Ω^L	22.2245	19.5020	16.3317	12.3742	6.2864
	$\Delta\Omega$	0	0.7456	1.7236	3.1830	6.2858
	Ω_{DI}	0	0.5363	1.2398	2.2895	4.5213
8	Ω^U	22.4877	20.4873	18.2691	15.7415	12.7211
	Ω^L	22.4877	19.7329	16.5251	12.5208	6.3609
	$\Delta\Omega$	0	0.7544	1.7440	3.2207	6.3602
	Ω_{DI}	0	0.5238	1.2109	2.2362	4.4161

Table 5 Effect of layer number on the dynamic instability with different tensile static load parameters ($a/b = 1$, $a/h = 10$, $E_1 / E_2 = 40$, $T_o / T_{cr} = 0.5$, $\alpha_D / \alpha_S = 0.3$, $\beta = 0$)

N		α_S				
		0	-0.2	-0.4	-0.6	-0.8
2	Ω^U	15.0818	16.7265	18.2233	19.6062	20.8978
	Ω^L	15.0818	16.3134	17.4584	18.5327	19.5481
	$\Delta\Omega$	0	0.4131	0.7650	1.0735	1.3497
	Ω_{DI}	0	0.9507	1.7607	2.4708	3.1065
4	Ω^U	21.4231	23.7594	25.8856	27.8500	29.6847
	Ω^L	21.4231	23.1727	24.7990	26.3252	27.7675
	$\Delta\Omega$	0	0.5867	1.0866	1.5249	1.9172
	Ω_{DI}	0	0.4712	0.8726	1.2246	1.5396
6	Ω^U	22.2245	24.6482	26.8539	28.8918	30.7951
	Ω^L	22.2245	24.0395	25.7267	27.3099	28.8062
	$\Delta\Omega$	0	0.6087	1.1272	1.5819	1.9889
	Ω_{DI}	0	0.4378	0.8108	1.1378	1.4306
8	Ω^U	22.4877	24.9400	27.1719	29.2339	31.1597
	Ω^L	22.4877	24.3241	26.0313	27.6332	29.1473
	$\Delta\Omega$	0	0.6159	1.1406	1.6006	2.0125
	Ω_{DI}	0	0.4276	0.7919	1.1114	1.3973

Table 6 Effect of layer number on the dynamic instability with different dynamic load parameters (a/b = 1, a/h = 10, E_1 / E_2 = 40, T_o / T_{cr} = 0.5, α_D / α_S = 0, β = 0)

N		α_D				
		0	-0.2	-0.4	-0.6	-0.8
2	Ω^U	15.0818	16.5212	17.8449	19.0770	20.2342
	Ω^L	15.0818	13.4896	11.6823	9.5386	6.7450
	$\Delta\Omega$	0	3.0317	6.1626	9.5384	13.4893
	Ω_{DI}	0	6.9778	14.1842	21.9541	31.0477
4	Ω^U	21.4231	23.4679	25.3482	27.0983	28.7421
	Ω^L	21.4231	19.1615	16.5943	13.5493	9.5809
	$\Delta\Omega$	0	4.3064	8.7538	13.5490	19.1612
	Ω_{DI}	0	3.4583	7.0298	10.8806	15.3875
6	Ω^U	22.2245	24.3457	26.2964	28.1120	29.8173
	Ω^L	22.2245	19.8782	17.2151	14.0561	9.9393
	$\Delta\Omega$	0	4.4675	9.0813	14.0559	19.8780
	Ω_{DI}	0	3.2134	6.5320	10.1101	14.2978
8	Ω^U	22.4877	24.6340	26.6077	28.4448	30.1703
	Ω^L	22.4877	20.1136	17.4189	14.2226	10.0570
	$\Delta\Omega$	0	4.5204	9.1888	14.2223	20.1133
	Ω_{DI}	0	3.1386	6.3800	9.8749	13.9652

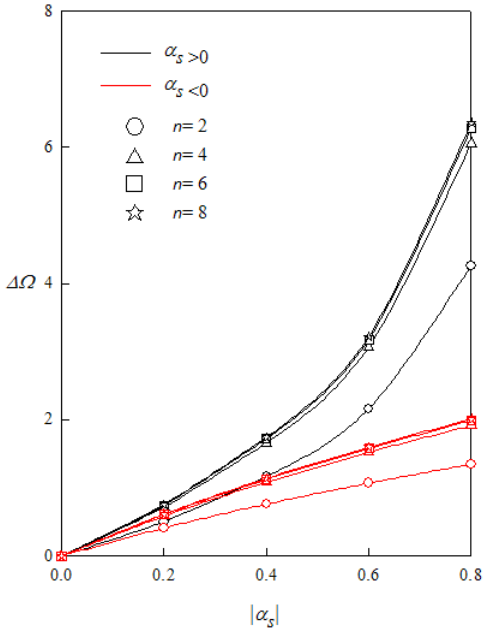

Fig. 1 Effect of static load parameters on instability region (a/b = 1, a/h = 10, T_o / T_{cr} = 0.5, α_D / α_S = 0.3, β = 0)

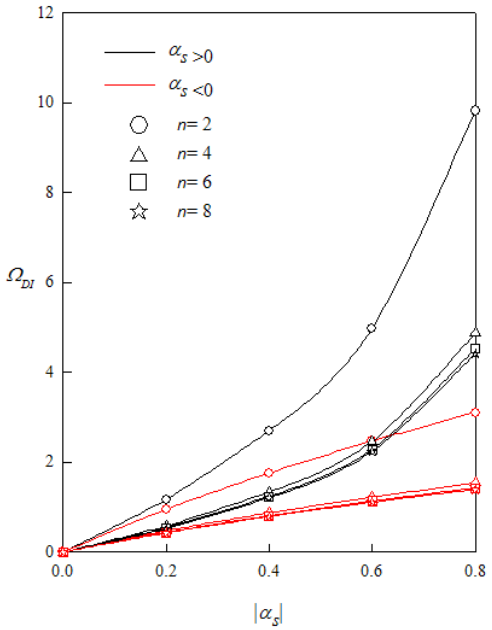

Fig. 2 Effect of dynamic load parameters on dynamic instability index ($a/b = 1$, $a/h = 10$, $T_o / T_{cr} = 0.5$, $\alpha_D / \alpha_S = 0.3$, $\beta = 0$)

static load parameters ($\alpha_S > 0$) decreases the excitation frequency but the tensile load ($\alpha_S < 0$) has the reverse trend. Furthermore, the compressive static load parameters produce a greater influence on the instability region and dynamic instability index than the tensile ones. As the dynamic load parameter increases, the upper excitation frequency increases, but lower excitation frequency decreases. The width of the unstable zone $\Delta\Omega$ increases with the increasing static and dynamic load, and the region is becoming much wider at the higher dynamic load parameter. The dynamic instability index Ω_{DI} is increased with the increase in static and dynamic load parameter. However, the dynamic load parameter has more apparent influence on dynamic instability index than the static load parameter. As shown in Figs. 1-2, the increasing layer number increases the width of the instability region and decreases the dynamic instability index. This is due to the fact that the increase in number of layer will increase the natural frequency and buckling load, which result in a decrease of dynamic instability index. Thus, the dynamic instability of laminate plates is significantly affected by the dynamic load parameter and layer number.

The effects of static and dynamic load parameters on the excitation frequency ratio Ω / ω_{nf} are given in Figs. 3 and 4, respectively. As can be seen, the primary instability region occurs in the vicinity of Ω equal to $2\omega_{nf}$, namely $\Omega / \omega_{nf} = 2$. The increasing static compressive load parameter decreases the upper and lower boundary of frequency ratio Ω / ω_{nf}, but the static tensile load parameter has a reverse effect. Meanwhile, the distance between the two boundaries becomes wider as the static load parameter increases. With the increase in dynamic load parameter, the upper excitation frequency ratio increases and the lower excitation frequency ratio decreases. From the comparison between the results in Figs. 3 and 4, the effect of dynamic load parameter on the excitation frequency ratio is more significant than that of static load parameter. Same behavior can also be observed for the laminated plates with different values of layer number, thermal

temperature and materials property. With variation in material, geometric size and thermal condition, both the natural frequency and exciation frequency will certainly change. However, the variation of the excitatation frequency ratio Ω / ω_{nf} against the respective static and dynamic load factor remains unchanged as shown in Figs. 3 and 4, while the material, geometric size or thermal condition is varied.

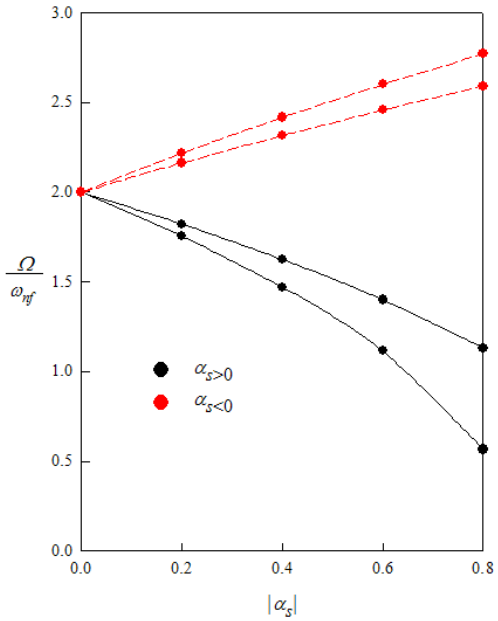

Fig. 3 Effect of static load parameters on Ω / ω_{nf} ($a/b = 1$, $a/h = 10$, $\alpha_D / \alpha_S = 0.3$, $\beta = 0$)

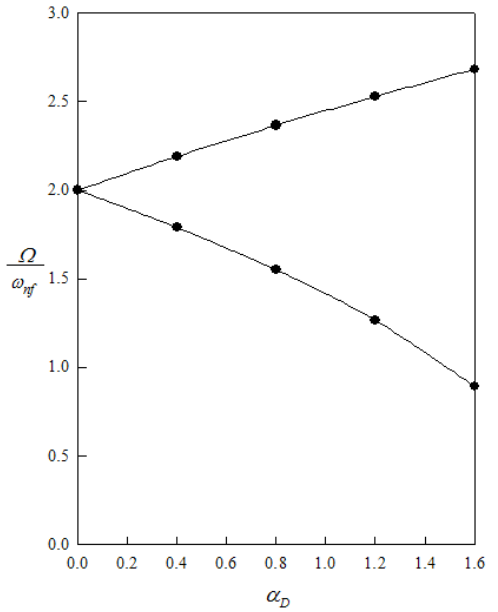

Fig. 4 Effect of dynamic load parameters on Ω / ω_{nf} ($a/b = 1$, $a/h = 10$, $\alpha_S = 0.1$, $\beta = 0$)

Table 7 Effect of compressive static load parameters on the dynamic instability under various temperature rise ($a/b = 1$, $a/h = 10$, $E_1 / E_2 = 40$, $N = 2$, $\alpha_D / \alpha_S = 0.3$, $\beta = 0$)

T_o / T_{cr}		α_S				
		0	0.2	0.4	0.6	0.8
0	Ω^U	21.3287	19.4314	17.3275	14.9301	12.0653
	Ω^L	21.3287	18.7158	15.6733	11.8753	6.0327
	$\Delta\Omega$	0	0.7155	1.6542	3.0548	6.0326
	Ω_{DI}	0	0.5823	1.3461	2.4859	4.9092
0.25	Ω^U	18.4712	16.8281	15.0061	12.9299	10.4490
	Ω^L	18.4712	16.2085	13.5736	10.2845	5.2248
	$\Delta\Omega$	0	0.6196	1.4325	2.6455	5.2242
	Ω_{DI}	0	0.7763	1.7948	3.3145	6.5453
0.5	Ω^U	15.0818	13.7402	12.2525	10.5573	8.5317
	Ω^L	15.0818	13.2342	11.0829	8.3973	4.2661
	$\Delta\Omega$	0	0.5059	1.1697	2.1600	4.2655
	Ω_{DI}	0	1.1645	2.6922	4.9716	9.8178
0.75	Ω^U	10.6646	9.7159	8.6640	7.4653	6.0330
	Ω^L	10.6646	9.3582	7.8369	5.9379	3.0168
	$\Delta\Omega$	0	0.3578	0.8271	1.5273	3.0161
	Ω_{DI}	0	2.3289	5.3842	9.9428	19.6345

Table 8 Effect of tensile static load parameters on the dynamic instability under various temperature rise ($a/b = 1$, $a/h = 10$, $\alpha_D / \alpha_S = 0.3$, $\beta = 0$)

T_o / T_{cr}		α_S				
		0	-0.2	-0.4	-0.6	-0.8
0	Ω^U	21.3287	23.6546	25.7715	27.7273	29.5539
	Ω^L	21.3287	23.0705	24.6897	26.2091	27.6451
	$\Delta\Omega$	0	0.5842	1.0818	1.5182	1.9088
	Ω_{DI}	0	0.4754	0.8803	1.2354	1.5533
0.25	Ω^U	18.4712	20.4856	22.3188	24.0125	25.5944
	Ω^L	18.4712	19.9797	21.3820	22.6978	23.9414
	$\Delta\Omega$	0	0.5059	0.9369	1.3148	1.6530
	Ω_{DI}	0	0.6338	1.1738	1.6472	2.0710
0.5	Ω^U	15.0818	16.7265	18.2233	19.6062	20.8978
	Ω^L	15.0818	16.3134	17.4584	18.5327	19.5481
	$\Delta\Omega$	0	0.4131	0.7650	1.0735	1.3497
	Ω_{DI}	0	0.9507	1.7607	2.4708	3.1065
0.75	Ω^U	10.6646	11.8275	12.8860	13.8639	14.7772
	Ω^L	10.6646	11.5355	12.3451	13.1048	13.8228
	$\Delta\Omega$	0	0.2921	0.5409	0.7591	0.9544
	Ω_{DI}	0	1.9014	3.5212	4.9415	6.2129

Table 9 Effect of dynamic load parameters on the dynamic instability under various temperature rise (a/b = 1, a/h = 10, α_D / α_S = 0.3, β = 0)

T_o / T_{cr}		α_D				
		0	0.4	0.8	1.2	1.6
0	Ω^U	21.3287	23.3644	25.2364	26.9789	28.6154
	Ω^L	21.3287	19.0770	16.5211	13.4895	9.5385
	$\Delta\Omega$	0	4.2874	8.7153	13.4894	19.0769
	Ω_{DI}	0	3.4890	7.0923	10.9773	15.5242
0.25	Ω^U	18.4712	20.2342	21.8554	23.3644	24.7817
	Ω^L	18.4712	16.5212	14.3078	11.6823	8.2608
	$\Delta\Omega$	0	3.7130	7.5476	11.6821	16.5209
	Ω_{DI}	0	4.6520	9.4563	14.6363	20.6988
0.5	Ω^U	15.0818	16.5212	17.8449	19.0770	20.2342
	Ω^L	15.0818	13.4896	11.6823	9.5386	6.7450
	$\Delta\Omega$	0	3.0317	6.1626	9.5384	13.4893
	Ω_{DI}	0	6.9778	14.1842	21.9541	31.0477
0.75	Ω^U	10.6646	11.6824	12.6184	13.4897	14.3079
	Ω^L	10.6646	9.5387	8.2608	6.7450	4.7696
	$\Delta\Omega$	0	2.1437	4.3576	6.7447	9.5383
	Ω_{DI}	0	13.9553	28.3676	43.9069	62.0934

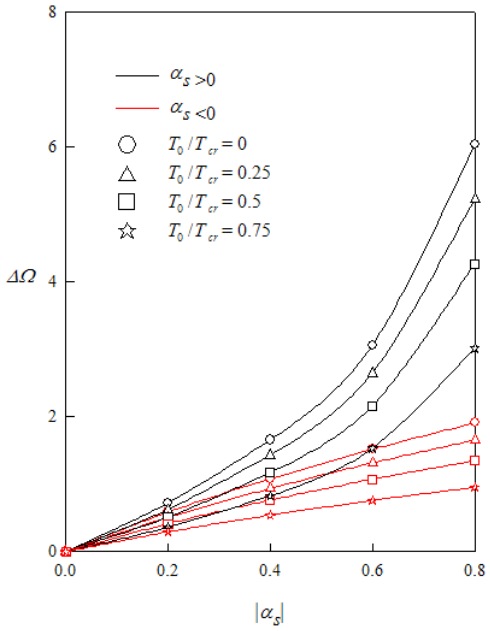

Fig. 5 Effect of static load parameters on instability region under uniform temperature rise (a/b = 1, a/h = 10, α_D / α_S = 0.3, β = 0)

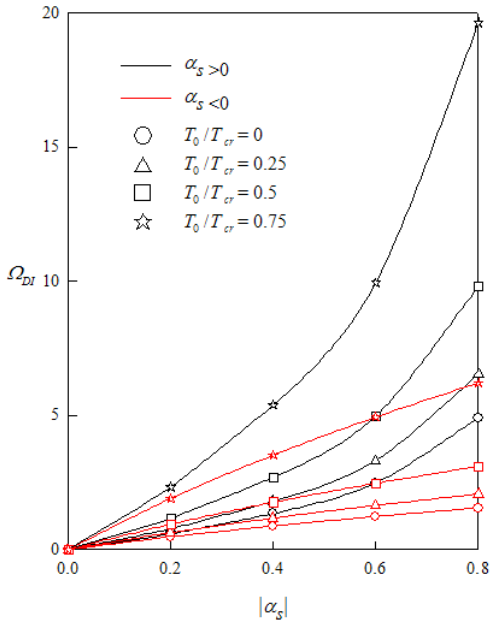

Fig. 6 Effect of static load parameters on dynamic instability index under uniform temperature rise ($a/b = 1$, $a/h = 10$, $\alpha_D / \alpha_S = 0.3$, $\beta = 0$)

Tables 7-9 present the effect of static and dynamic load parameter on the excitation frequency, instability region and dynamic instability index for laminated plates with different uniform temperature rise. As expected, the increase of static and dynamic load parameter always increases the dynamic instability index and instability region of laminated plates regardless of the temperature rise. However, the increasing uniform temperature rise decreases the excitation frequency of the instability region, but increases the dynamic instability index. Moreover, higher temperature rise has a more apparent influence on the dynamic instability than the dynamic load parameter. Hence, the laminated plate becomes more dynamically unstable when it is subjected to a higher temperature rise.

Figs. 5-6 show the effect of static loading type on the instability region and dynamic instability index of laminated plates with various uniform temperature rise. As can be observed, the static load parameter $|\alpha_S|$ always increases the instability region and dynamic instability index. However, the increase in temperature rise will increase the dynamic instability index and shift the instability region to lower excitation frequency. Therefore, the higher the temperature rise and compressive static load is, more dynamically unstable the laminated plate is.

Tables 10-12 show the dynamic stability of laminated plates with different modulus ratios. The excitation frequency and instability region are increased and dynamic instability index decreased when the modulus ratio is increased. The laminated plate is becoming more dynamically unstable as the modulus ratio decreases. The effects of the different static load types on the instability region and dynamic instability index for laminated plates with various modulus ratios are given in Figs. 7 and 8. It can be found that the instability region and dynamic instability index are enlarged significantly with the increasing compressive static load. Thus, the laminated plate with lower modulus ratio under compressive static load is more dynamically unstable than that with higher modulus ratio under tensile one.

Table 10 Effect of modulus ratio on the dynamic instability with different compressive static load parameters ($a/b = 1$, $a/h = 10$, $T_o / T_{cr} = 0.5$, $\alpha_D / \alpha_S = 0.3$, $\beta = 0$)

E_1 / E_2		α_D				
		0	0.2	0.4	0.6	0.8
5	Ω^U	10.0719	9.1760	8.1825	7.0504	5.6975
	Ω^L	10.0719	8.8381	7.4013	5.6078	2.8487
	$\Delta\Omega$	0	0.3379	0.7812	1.4425	2.8488
	Ω_{DI}	0	2.6111	6.0365	11.1475	22.0146
10	Ω^U	11.0511	10.0681	8.9780	7.7358	6.2515
	Ω^L	11.0511	9.6973	8.1209	6.1530	3.1258
	$\Delta\Omega$	0	0.3707	0.8571	1.5828	3.1257
	Ω_{DI}	0	2.1688	5.0141	9.2595	18.2859
20	Ω^U	12.6239	11.5009	10.2557	8.8368	7.1413
	Ω^L	12.6239	11.0774	9.2767	7.0288	3.5709
	$\Delta\Omega$	0	0.4235	0.9790	1.8080	3.5704
	Ω_{DI}	0	1.6621	3.8426	7.0961	14.0132
40	Ω^U	22.4877	20.4873	18.2691	15.7415	12.7211
	Ω^L	22.4877	19.7329	16.5251	12.5208	6.3609
	$\Delta\Omega$	0	0.7544	1.7440	3.2207	6.3602
	Ω_{DI}	0	0.5238	1.2109	2.2362	4.4161

Table 11 Effect of layer number on the dynamic instability with different tensile static load parameters ($a/b = 1$, $a/h = 10$, $\alpha_D / \alpha_S = 0.3$, $\beta = 0$)

E_1 / E_2		α_S				
		0	0.2	0.4	0.6	0.8
5	Ω^U	10.0719	11.1703	12.1700	13.0935	13.9561
	Ω^L	10.0719	10.8945	11.6591	12.3766	13.0547
	$\Delta\Omega$	0	0.2759	0.5109	0.7169	0.9014
	Ω_{DI}	0	2.1317	3.9478	5.5401	6.9655
10	Ω^U	11.0511	12.2563	13.3531	14.3665	15.3129
	Ω^L	11.0511	11.9536	12.7926	13.5799	14.3239
	$\Delta\Omega$	0	0.3027	0.5605	0.7866	0.9890
	Ω_{DI}	0	1.7707	3.2792	4.6018	5.7858
20	Ω^U	12.6239	14.0005	15.2534	16.4110	17.4921
	Ω^L	12.6239	13.6548	14.6131	15.5124	16.3623
	$\Delta\Omega$	0	0.3457	0.6403	0.8985	1.1297
	Ω_{DI}	0	1.3570	2.5130	3.5267	4.4340
40	Ω^U	22.4877	24.9400	27.1719	29.2339	31.1597
	Ω^L	22.4877	24.3241	26.0313	27.6332	29.1473
	$\Delta\Omega$		0.6159	1.1406	1.6006	2.0125
	Ω_{DI}		0.4276	0.7919	1.1114	1.3973

Table 12 Effect of layer number on the dynamic instability with different dynamic load parameters ($a/b = 1$, $a/h = 10$, $\alpha_S = 0$, $\beta = 0$)

E_1 / E_2		α_D				
		0	0.4	0.8	1.2	1.6
5	Ω^U	10.0719	11.0333	11.9173	12.7401	13.5129
	Ω^L	10.0719	9.0086	7.8017	6.3700	4.5043
	$\Delta\Omega$	0	2.0246	4.1156	6.3701	9.0086
	Ω_{DI}	0	15.6458	31.8040	49.2258	69.6158
10	Ω^U	11.0511	12.1059	13.0759	13.9787	14.8266
	Ω^L	11.0511	9.8844	8.5602	6.9894	4.9423
	$\Delta\Omega$	0	2.2215	4.5157	6.9893	9.8844
	Ω_{DI}	0	12.9960	26.4176	40.8889	57.8255
20	Ω^U	12.6239	13.8287	14.9367	15.9680	16.9366
	Ω^L	12.6239	11.2911	9.7784	7.9841	5.6457
	$\Delta\Omega$	0	2.5376	5.1583	7.9839	11.2909
	Ω_{DI}	0	9.9597	20.2455	31.3356	44.3152
40	Ω^U	22.4877	24.6340	26.6077	28.4448	30.1703
	Ω^L	22.4877	20.1136	17.4189	14.2226	10.0570
	$\Delta\Omega$	0	4.5204	9.1888	14.2223	20.1133
	Ω_{DI}	0	3.1386	6.3800	9.8749	13.9652

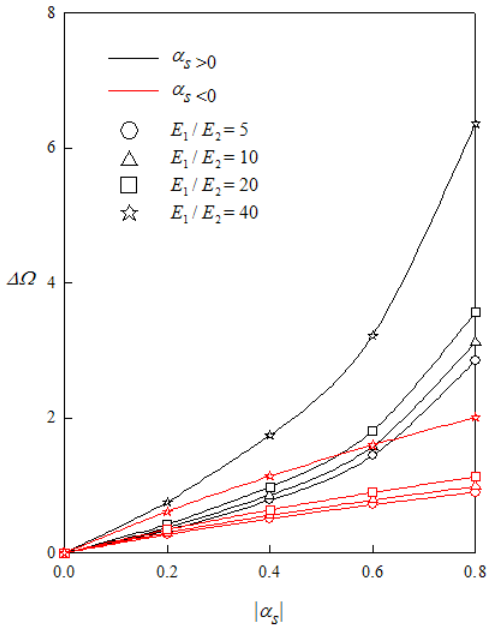

Fig. 7 Effect of static load parameters on instability region under various modulus ratio ($a/b = 1$, $a/h = 10$, $\alpha_D / \alpha_S = 0.3$, $\beta = 0$)

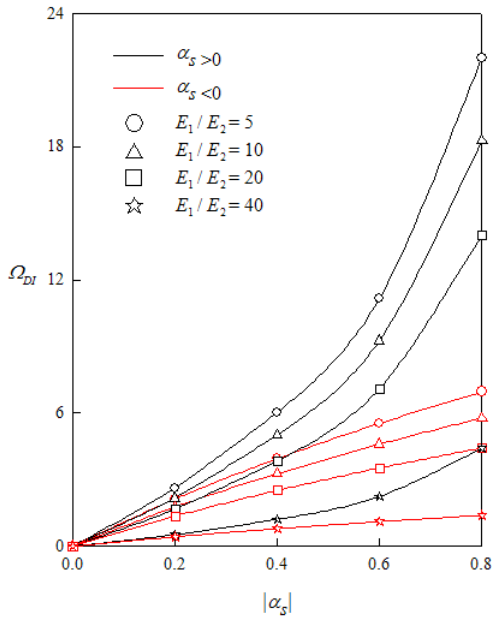

Fig. 8 Effect of static load parameters on dynamic instability index under various modulus ratio ($a/b = 1$, $a/h = 10$, $T_o / T_{cr} = 0.5$, $\alpha_D / \alpha_S = 0.3$, $\beta = 0$)

Table 13 Effect of gradient temperature on the dynamic instability Ω_{DI} with different static load parameters ($a/b = 1$, $a/h = 10$, $\alpha_D / \alpha_S = 0.3$, $n = 2$, $E_1 / E_2 = 10$)

T_o / T_{cr}	T_g / T_o	α_S				
		0	0.2	0.4	0.6	0.8
0	0	0	1.0845	2.5072	4.6299	9.1434
0.25	0	0	1.4459	3.3428	6.1731	12.1909
	10	0	1.4463	3.3439	6.1763	12.2063
	20	0	1.4474	3.3473	6.1860	12.2530
	40	0	1.4518	3.3611	6.2250	12.4462
0.5	0	0	2.1688	5.0141	9.2595	18.2859
	10	0	2.1721	5.0243	9.2884	18.4262
	20	0	2.1821	5.0553	9.3769	18.8713
	40	0	2.2235	5.1856	9.7591	21.1629
0.75	0	0	4.3375	10.0277	18.5179	36.5684
	10	0	4.3673	10.1205	18.7826	37.8948
	20	0	4.4609	10.4157	19.6529	43.3141
	40	0	4.9081	11.9308	23.0649	65.357

The influence of static and dynamic load parameters on the dynamic instability index of laminated plates under linear temperature gradient rise is presented in Tables 13 and 14. The effect of linear temperature gradient rise T_g on the dynamic stability is less apparent than uniform

Table 14 Effect of gradient temperature on the dynamic instability Ω_{DI} with different dynamic load parameters ($a/b = 1$, $a/h = 10$, $\alpha_S = 0$, $n = 2$, $E_1 / E_2 = 10$)

T_o / T_{cr}	T_g / T_o	α_S				
		0	0.4	0.8	1.2	1.6
0	0	0	6.4982	13.2093	20.4452	28.9138
0.25	0	0	8.6641	17.6120	27.2597	38.5510
	10	0	8.6659	17.6159	27.2666	38.5640
	20	0	8.6713	17.6276	27.2872	38.6031
	40	0	8.6929	17.6745	27.3706	38.7611
0.5	0	0	12.9960	26.4176	40.8889	57.8255
	10	0	13.0121	26.4526	40.9510	57.9428
	20	0	13.0608	26.5586	41.1393	58.3011
	40	0	13.2615	26.9969	41.9257	59.8427
0.75	0	0	25.9907	52.8325	81.7734	115.6446
	10	0	26.1365	53.1498	82.3374	116.7167
	20	0	26.5900	54.1404	84.1175	120.2256
	40	0	28.6861	58.8167	93.0203	144.4015

temperature rise T_o. Hence, the lower temperature gradient and smaller load parameter has a minor influence on the dynamic instability of the laminated plate. The effects of static load type and linear temperature gradient rise on the dynamic instability index of laminate plates under various dynamic loads are presented in Table 15. The tensile static load reduces the effect of the temperature gradient and dynamic load on the dynamic stability but the compressive static load has an opposite influence on the dynamic instability index. Meanwhile, the increasing temperature gradient causes a greater change in the dynamic instability index for the laminated plate under the compressive static load. Tables 16 and 17 give the effect of the bending stress coefficient β on the dynamic instability. The dynamic instability index increases with the increases in bending stress ratio, especially for the laminated plate under the compressive load and a higher gradient temperature. The laminated plate is more dynamically unstable when it is subjected to the compressive load, higher bending stress and temperature gradient.

Table 15 Effect of static load type and gradient temperature on the dynamic instability Ω_{DI} with different dynamic load parameters ($a/b = 1$, $a/h = 10$, $n = 2$, $E_1 / E_2 = 10$, $T_o / T_{cr} = 0.75$)

α_S	T_g / T_o	α_S					
		0	0.2	0.4	0.6	0.8	1.0
-0.4	0	0	10.9345	21.9112	32.9745	44.1727	55.5611
	10	0	10.9774	21.9979	33.1068	44.3533	55.7943
	20	0	11.1095	22.2648	33.5139	44.9098	56.5135
	40	0	11.6921	23.4435	35.3170	47.3833	59.7269

Table 15 Continued

0	0	0	12.9458	25.9907	39.2431	52.8325	66.9281
	10	0	13.0173	26.1365	39.4694	53.1498	67.3539
	20	0	13.2394	26.5900	40.1740	54.1404	68.6888
	40	0	14.2620	28.6861	43.4573	58.8167	75.1249
0.4	0	0	16.7505	33.8715	51.8419	71.4719	94.7175
	10	0	16.9071	34.2029	52.3955	72.3633	96.3371
	20	0	17.4052	35.2628	54.1846	75.3158	102.1926
	40	0	19.9755	40.8908	64.3859	93.0182	118.924

Table 16 Effect of the bending stress ratio on the Ω_{DI} dynamic instability with different gradient temperature ($a/b = 1$, $a/h = 10$, $\alpha_D / \alpha_S = 0.3$, $n = 2$, $E_1 / E_2 = 10$, $T_o / T_{cr} = 0.75$)

α_S	T_g / T_o	β				
		0	10	20	30	40
-0.4	0	6.5580	6.5521	6.5344	6.5049	6.4636
	10	6.6304	6.6658	6.6894	6.7012	6.7012
	20	6.8574	6.9370	7.0045	7.0600	7.1037
	40	7.9499	8.1428	8.3224	8.4889	8.6425
0.4	0	10.0277	10.0391	10.0734	10.1305	10.2108
	10	10.1383	10.2486	10.3827	10.5410	10.7238
	20	10.4856	10.7026	10.9455	11.2151	11.5124
	40	12.1560	12.6496	13.1791	13.7465	14.3543

Table 17 Effect of static load type and dynamic load parameters on the dynamic instability Ω_{DI} under various bending stress ratio ($a/b = 1$, $a/h = 10$, $\alpha_S = 0$, $n = 2$, $E_1 / E_2 = 10$, $T_o / T_{cr} = 0.75$, $T_g / T_o = 40$)

α_S	T_g / T_o	β				
		0	10	20	30	40
-0.4	0.2	13.2552	13.5772	13.8769	14.1549	14.4115
	0.4	26.5617	27.2093	27.8130	28.3737	28.8920
	0.8	53.5479	54.8744	56.1174	57.2784	58.3589
0.4	0.2	20.3058	21.1355	22.0266	22.9829	24.0088
	0.4	41.0607	42.7918	44.6630	46.6861	48.8751
	0.8	86.6420	90.9986	95.9296	101.5897	108.2341

5. Conclusions

The dynamic stability of laminate plates subjected to thermal load and periodic dynamic loads has been investigated. The dynamic instability is sensitive to the thermal load and periodic dynamic load. Based on above discussions, the preliminary results are summarized as follows:

1. The excitation frequency, instability region and dynamic instability index are significantly affected by the static load component, dynamic load amplitude, layer number, modulus ratio and uniform temperature rise. They are slightly affected by the temperature gradient rise and bending stress.
2. The dynamic instability index increases with the increasing static loading, dynamic loading and temperature rise, but reduces with the increase in the number of layer and modulus ratio. The compressive static load has a more apparent influence than tensile load on the dynamic instability.
3. Though the natural frequency and exciation frequency will change with variation in material, geometric size and thermal condition, the variation of the excitatation frequency ratio against the respective static and dynamic load factor remains unchanged.

Acknowledgements

This research was supported by the National Science Council through the grant NSC-98-2221-E-262 -009 -MY3.

References

Al-Huniti, N.S. and Al-Nimr, M.A. (2004), "Dynamic thermoelastic response of a heated thin composite plate using the hyperbolic heat conduction model", *Int. J. Heat Tech.*, **22**(1), 179-185.

Bolotin, V.V. (1964), *The Dynamic Stability of Elastic Systems*, Holden-Day, San Francisco.

Evan-Ivanowski, R.M. (1976), *Resonance Oscillations in Mechanical Systems*, Elsevier, Amsterdam.

Chakrabarti, A. (2008), "An efficient FE model for dynamic instability analysis of imperfect composite laminates", *Struct. Eng. Mech., Int. J.*, **30**(3), 383-386.

Chen, C.S. (2007), "The nonlinear vibration of an initially stressed laminated plate", *Compos. Part B: Eng.*, **38**(4), 437-447.

Chen, C.S., Chen, W.R. and Chien, R.D. (2009), "Stability of parametric vibrations of hybrid laminated plates", *Eur. J. Mech. A/Solids*, **28**(2), 329-337.

Chen, L.W. and Yang, J.Y. (1990), "Dynamic stability of laminated composite plates by the finite element method", *Comput. Struct.*, **36**(5), 845-851.

Dey, P. and Singha, M.K. (2006), "Dynamic stability analysis of composite skew plates subjected to periodic in-plane load", *Thin-Walled Struct.*, **44**(9), 937-942.

Fares, M.E., Youssif, Y.G. and Hafiz, M.A. (2004), "Structural and control optimization for maximum thermal buckling and minimum dynamic response of composite laminated plates", *Int. J. Solids Struct.*, **41**(3-4), 1005-1019.

Heidary, F. and Eslami, M.R. (2004), "Dynamic analysis of distributed piezothermoelastic composite plate using first-order shear deformation theory", *J. Thermal Stresses*, **27**(7), 587-605.

Liu, C.F. and Huang, C.H. (1996), "Free vibration of composite laminated plates subjected to temperature changes", *Comput. Struct.*, **60**(1), 95-101.

Makhecha, D.P., Ganapathi, M. and Patel, B.P. (2001), "Dynamic analysis of laminated composite plates subjected to thermal/mechanical loads using an accurate theory", *Compos. Struct.*, **51**(3), 221-236.

Matsunaga, H. (2005), "Thermal buckling of cross-ply laminated composite and sandwich plates according to a global higher order deformation theory", *Compos. Struct.*, **68**(4), 439-454.

Moradi, S. and Mansouri, M.H. (2012), "Thermal buckling analysis of shear deformable laminatedorthotropic plates by differential quadrature", *Steel Compos. Struct., Int. J.*, **12**(2), 129-147.

Patel, S.N., Datta, P.K. and Sheikh, A.H. (2009), "Parametric study on the dynamic instability behavior of

laminated composite stiffened plate", *J. Eng. Mech.*, **135**(11), 1331-1341.
Shariyat, M. (2009), "Dynamic buckling of imperfect laminated plates with piezoelectric sensors and actuators subjected to thermo-electro-mechanical loadings, considering the temperature-dependency of the material properties", *Compos. Struct.*, **88**(2), 228-239.
Shen, H.S., Zheng, J.J. and Huang, X.L. (2003), "Dynamic response of shear deformable laminated plates under thermomechanical loading and resting on elastic foundations", *Compos. Struct.*, **60**(1), 57-66.
Shukla, K.K. and Nath, Y. (2002), "Buckling of laminated composite rectangular plates under transient thermal loading", *J. Appl. Mech. Trans., ASME*, **69**(5), 684-692.
Tylikowski, A. (2003), "Shear deformation effects on thermally induced instability of laminated plates", *J. Thermal Stresses*, **26**(11-12), 1251-1261.
Topal, U. (2012), "Thermal buckling load optimization of laminated plates with different intermediate line supports", *Steel Compos. Struct., Int. J.*, **13**(3), 207-223.
Wang, S. and Dawe, D.J. (2002), "Dynamic instability of composite laminated rectangular plates and prismatic plate structures", *Comput. Meth. Appl. Mech. Eng.*, **191**(17-18), 1791-1826.

CC